ChemComm

Accepted Manuscript

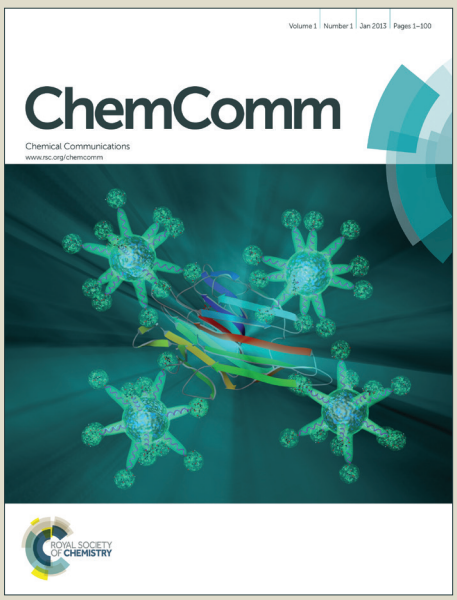

ROYAL SOCIETY OF CHEMISTRY

www.rsc.org/chemcomm

Journal Name ChemComm Dynamic Article Links ►

Cite this: DOI: 10.1039/c0xx00000x

www.rsc.org/xxxxxx

ARTICLE TYPE

Facile electrochemical synthesis of titanium dioxide dendrites and its electrochemical properties

Sang Ha Lee, Hyuck Lee, Misuk Cho, and *Youngkwan Lee

Received (in XXX, XXX) Xth XXXXXXXXX 20XX, Accepted Xth XXXXXXXXX 20XX
DOI: 10.1039/b000000x

Titanium dioxide (TiO_2) dendrites were successfully prepared by a simple electrochemical deposition technique under acidic solution. The TiO_2 dendrites showed outstanding electrochemical properties.

Titanium dioxide (TiO_2) is a widely utilized, multifunctional material in both research and industrial fields due to its various applications such as photocatalysis, photovoltaic cells, gas sensors, electrochromic devices, and Li ion batteries with inherent chemical stability, transparency, low cost, and minimal toxicity [1]. However, the specific tailoring of the electrochemical properties of TiO_2 still offers a great deal of room for investigation. In order to control the electrochemical properties of TiO_2, extensive research has focused on the formation of nanostructured materials. A various nanostructures, such as 1D, 2D and 3D structures [2], have become very attractive for various applications due to their band gap control, high accessible area, and efficient diffusion path of charge carriers. In the past decade, the fabrication of TiO_2 nanostructures by electrochemical anodization of titanium was investigated by many researchers due to its simplicity in which titanium foil was used as a substrate and the tube dimension was available at only at a limited scale [3].

However, even for the film with dense arrays of nanostructure, the overall surface area developed by these structures was insufficient, and the growth of multiscale hierarchical structures has been proposed [4]. These hierarchical assemblies combine characteristic aspects of nanometer and micrometer-sized building blocks, provide higher surface area, and an efficient path of transporting the ions and electrons [5]. As a result, considerable research has been done on the preparation of hierarchical structures, and these results showed high performance for dye-sensitized solar cells, photocatalysts, or lithium battery anodes [6]. Nevertheless, these hierarchical structures were manufactured by the complex, expensive, and often hard preparation of the template, and it is important to develop a facile, low-cost, and mild method.

Electrochemical deposition method has been of considerable interest due to its many advantages such as simplicity, low cost, uniformity, and easy-to-control thickness. Despite these advantages, only few attempts have been made to deposit TiO_2 films via this technique comparatively to other methods. Recently, Hu et al. successfully controlled morphology and thickness of TiO_2 film by using various electrochemical deposition methods including galvanostatic, potentiostatic, and pulse-rest mode [7], however, no work was done for the synthesis dendritic structured TiO_2 via an electrochemical deposition.

In this study, TiO_2 dendrite, one type of hierarchical structures, was obtained by the pulse reverse potential (PRP) electrodeposition under acidic solution. We investigated the influence of various electrochemical deposition conditions on the dendrite formation. Furthermore, the mechanism and kinetics of dendrite formation were studied by using an electrochemical quartz crystal microbalance (QCM), and the electrochemical properties of the TiO_2 dendrite were investigated by cyclic voltammetry.

The mechanism of preparation of TiO_2 films by cathodic deposition with $TiCl_3$ has been postulated by Hu [6]. At first, $TiCl_3$ was completely oxidised to $(TiOH)^{3+}$ with the addition of H_2O_2. Further olation of TiOH forms dimers and polymeric oxy-hydroxyl Ti precipitates, which will be converted to TiO_2 through dehydration. The generation of concentrated OH^- for TiO_2 deposition is in the negative potential regions with NO_3^- ions. The mechanism can be described simply as follows.

$$2NO_3^- + 6H_2O + 10e^- \rightarrow N_2 + 12OH^- \quad (1)$$
$$NO_3^- + 6H_2O + 8e^- \rightarrow NH_3 + 9OH^- \quad (2)$$

In the electrochemical deposition technique, it is well known that the morphology of the produced materials is greatly dependent on the pattern of the applied potential. In this study, we applied a pulse technique to produce dendritic TiO_2. A TiO_2 film was produced by using two different methods of applied potentials, a continuous potential (CP) at -1.6 V and a repeated alternating pulse reverse potential at -1.6/+1.6 V (Figure S1).

As shown in Figure 1, the morphologies of TiO_2 synthesised by CP and PRP were observed with a scanning electron microscope (SEM). In the case of CP mode, a typical bulk film with large cracks was obtained (Figure 1a). It is well known that the cathodic electrodeposition of TiO_2 produces a bulk film structure.[8] In the case of PRP, a dendrite structure with an average branch diameter of about 50 nm was obtained (Figure 1h). The growth mechanism of dendrite structures can be explained by using a diffusion-limited aggregation (DLA)

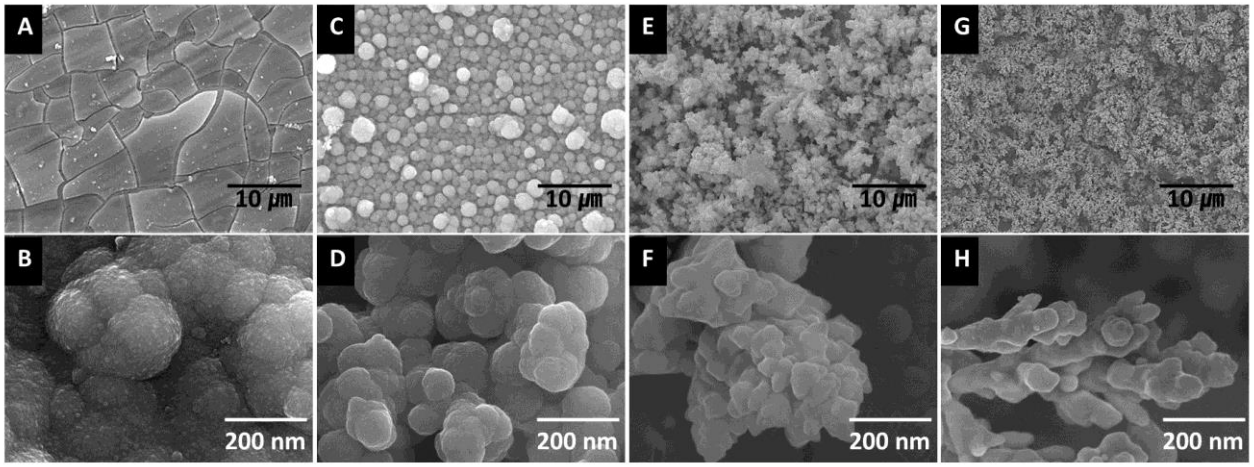

Fig. 1 SEM images of TiO_2 synthesized under (a-b) CP and (c-h) PP with a various pulse potential: (c-d) -1.6 V/ 0 V; (e-f) -1.6 V/1.0 V; (g-h) -1.6 V/ 1.6 V, at low magnification (a,c,e,g) and high magnification (b,d,f,h).

model.[9] Initially, the TiO_2 precursor aggregated each other, and primary TiO_2 particles are formed during cathodic (-1.6 V) deposition. During the positive potential (+1.6 V), the Ti(IV) hydroxyl species receded from the vicinity of the working electrode due to the positively applied electric field.[10] This phenomenon induced the low concentration of Ti(IV) hydroxyl species on the surface of the electrode. In the next cathodic deposition period, the Ti(IV) hydroxyl species adsorbed at the TiO_2 cluster, where the growth occurred at the tips and stems of branches to yield the dendrite structure. Furthermore, during the positive potential, NO_3^- ions might be supplied to electrode surface and reduced to OH^- ions when the negative potential is applied which will react with Ti(IV) to form Ti oxide. As a result, the concentration of Ti(IV) at the electrode/electrolyte interface decreased with the cathodic reduction of nitrate ions. A concentration gradient of Ti(IV) will favor the diffusion of Ti(IV) to the vicinity of electrode surface. The intensity of the positive potential affects the concentration of Ti(IV) at the electrode surface, which strongly influenced the resulting dendrite structure (Figures 1(c-h)). It is clearly observed that TiO_2 prepared by applying a higher positive potential shows a sharper dendrite structure. This result may be due to a lower concentration of Ti hydroxyl species in the vicinity of the electrode resulting from a higher electric field [11].

Furthermore, in an electrodeposition process, hydrogen and nitrogen bubbles were continuously produced at the substrate due to the reduction of NO_3^- ions and H^+ ions at negative potential, and the gas evolution may assist the formation of dendritic structure [12]. The morphologies of TiO_2, according to the rate of hydrogen bubble formation, were also observed by varying the pH condition (Figure S3). As the pH of reaction solution became lower, the stem and branch were thinner, and the dendrite structure was less dense due to the large amount of hydrogen gas evolution.

In order to confirm the pattern of weight increase during electrodeposition, QCM analysis was performed (Figure 2). Variation of deposited weight was calculated from frequency with the following equation [13].

$$\text{Weight (g)} = \Delta\text{frequency} \times (-1.3)\ \text{ng/Hz}$$

In the case of CP, the mass of deposited TiO_2 continuously increased, and 8.5 μgcm^{-2} was deposited for 7 sec.

In the PRP deposition, the deposited weight increased at -1.6 V and then decreased at 1.6 V. The alternating gain and loss of mass was repeated, and the deposited amount was 6.5 μg for 7 sec (Figure 2a). Using QCM analysis, the mechanism of dendrite formation with the PRP method was clearly observed. The weight increase of TiO_2 was further monitored during a longer period of time (Figure 2b). Initially, the rate of weight increase was slightly higher for CP; however, the rate was reversed after 10 min. So, the PRP method allowed a much higher amount of TiO_2 (1.20 mg) growth than the CP method (0.69 mg) after 50 min. This result might be due to the increased surface area of TiO_2 dendrites (Figure S4), which will allow for more active sites for growth. In the case of the CP method, the TiO_2 film was initially formed on the electrode surface, and the thickness of TiO_2 film slowly increased. In the case of the PRP method, the mass increase and decrease were repeated during alternating negative/positive pulse process (Figure 2c), which might be due to the adsorption/ deposition and desorption of the Ti(IV) hydroxyl species, respectively. In order to further examine the mechanism, QCM study was conducted using Ti(IV) hydroxyl species only (without KNO_3). In this case, repeated mass increase and decrease was also observed, however, the deposition of TiO_2 was not found, because the support of OH^- ions was not available. So the reason for the weight decrease during positive potential could be explained by desorption of Ti(IV) hydroxyl species.

It is well known that the cathodically deposited TiO_2 has plenty of hydroxyl groups, and dehydration should occur during an annealing process. In order to confirm the structural evolution of crystalline TiO_2, an as-deposited electrode was annealed at 450 ℃ for 4 hours, and X-ray photoelectron spectroscopy (XPS) and X-ray diffraction (XRD) measurements were conducted to investigate the compositions and crystal structure of the electrode. Figure S6(a) shows the fully-scanned XPS spectrum of the TiO_2 dendrite after annealing. The overview spectrum demonstrated that Ti and O existed in the TiO_2 dendrite electrode, where

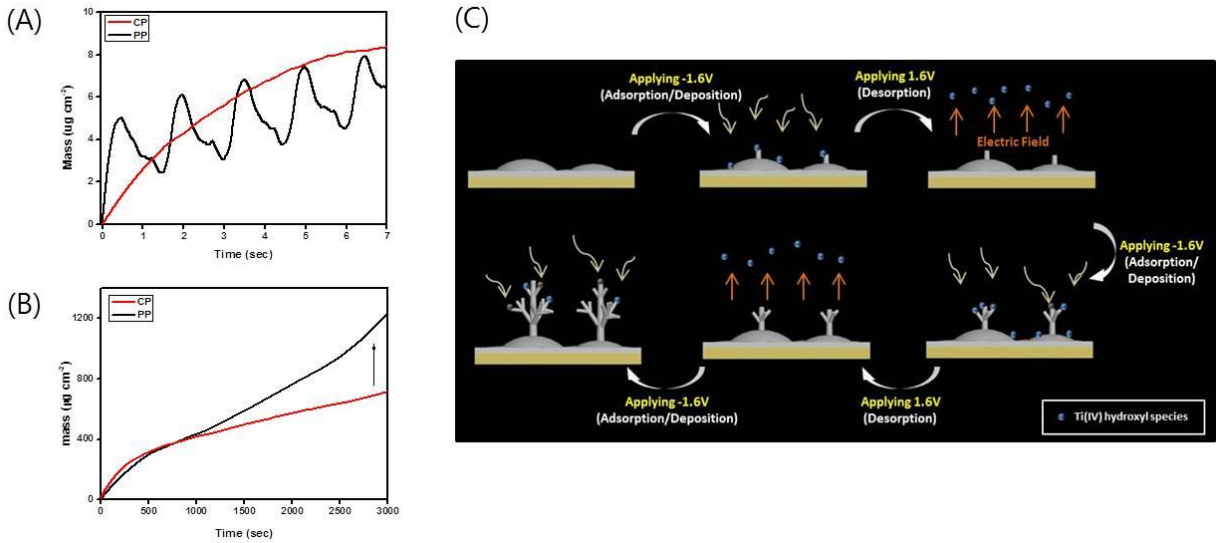

Fig. 2 (a-b) Weight increase of TiO_2 as a function of time: (a) from 0 to 7 sec; (b) from 0 to 3000 sec; (c) Schematic illustration of the formation of TiO_2 dendrite

Ti and O might be from TiO_2. Figure S6(b) provides the curve fitting of a Ti 2p XPS spectrum, in which two peaks that are attributed to Ti 2p3/2 and Ti 2p1/2 are clearly seen at 459.5 and 465.5 eV, respectively, and are well matched with Ti^{4+}.[14] Figure S6(c) represents the curve fitting of an O 1s spectrum. Two resolved peaks at 529.8 eV and 533.0 eV binding energies can tentatively be assigned to Ti-O-Ti (lattice O) and absorbed water, respectively.[15] Peak positions in the XRD pattern (Figure S6(d)) of the TiO_2 dendrite confirmed the fabrication of anatase and rutile structure (JCPDS No. 78-2486 and No. 21-1276). It is remarkable that the morphology of the TiO_2 dendrite was maintained during the annealing process (Figure S7).

To characterise the electrochemical properties of the TiO_2 dendrite, a cyclic voltammetry (CV) test was performed, as shown in Figure 3. All of these CV curves exhibited a quasi-rectangular shape without obvious redox peaks, thereby indicating the as-prepared samples displayed ideal double layer capacitor characteristics with a charge/discharge process. TiO_2 dendrites exhibited higher specific capacitance than the film at the same scan rates (Figure 3a). Notably, the CV curves of TiO_2 dendrite maintained a rectangular-like shape without distinct distortion even at 1000 mVs^{-1} (Figure 3b), thus demonstrating excellent capacitive behaviour and small equivalent series resistance with rapid charging/discharging characteristics.[16] Figure 3c shows the specific and areal capacitance of the TiO_2 film and dendrites as a function of the scan rate. The areal capacitance of TiO_2 film and dendrites at a scan rate of 5 mVs^{-1} reached as high as 2.0 and 34.2 $mFcm^{-2}$, respectively. As the scan rate increased up to 1000 mVs^{-1}, TiO_2 dendrites still retained a high capacitance of 10.3 $mFcm^{-2}$. Even though the electrode was fabricated by simple electrodeposition, the areal capacitance of TiO_2 dendrites was comparable to other works. Many different types of TiO_2 have been reported; however, the capacitance is much lower than that of TiO_2 dendrite (Table 1). The enhanced capacitance might be achieved from a dendrite structure that allows for effective material utilization due to their large surface area and facile access to the electrolyte. The cyclic stability test was also conducted at a scan rate of 50 mVs^{-1}, and the results are presented in Figure 3d. It is interesting to find that about 87 % of the initial capacitance of 15.3 $mFcm^{-2}$ for the TiO_2 dendrites was retained after 2,000 cycles, therefore indicating good cycle stability of TiO_2 dendrites.

In summary, we demonstrated that TiO_2 dendrites were electrochemically deposited by applying an alternating (-/+ 1.6 V) pulse potential. Dendrites were grown through a repeated process of adsorption/deposition and desorption during alternating potential pulses, which were confirmed by QCM analysis. In contrast to the TiO_2 film, TiO_2 dendrites showed excellent electrochemical properties 34.2 $mFcm^{-2}$ and 10.3 $mFcm^{-2}$ at 5 mVs^{-1} and 1000 mVs^{-1}, respectively. TiO_2 dendrite might be applied in many other applications such as photocatalysis, photovoltaic cells, gas sensors, and lithium ion batteries.

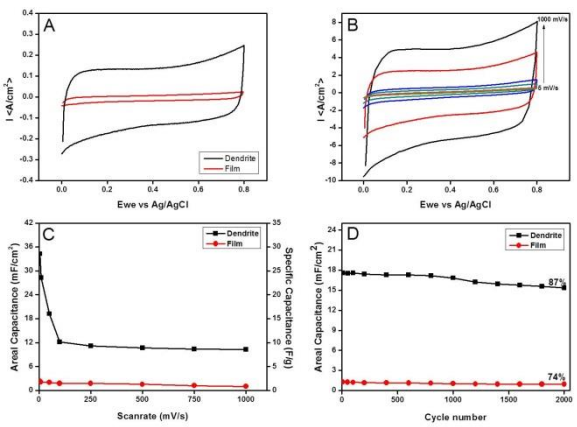

Fig. 3 (a) Cyclic voltammetry of the CP and PRP at 10 mVs^{-1}, (b) Cyclic voltammetry of TiO_2 prepared by PRP according to scan rate, (c) Areal and specific capacitances of the TiO_2 film and dendrite as a function of scan rate, (d) Areal capacitances of the TiO_2 film and dendrite as a function of cycle number

Cite this: DOI: 10.1039/c0xx00000x

www.rsc.org/xxxxxx

ARTICLE TYPE

Table 1 Comparison of the performance of various titanium oxide electrodes.

Materials	Method	Analysis condition		Areal capacitance ($mFcm^{-2}$)	Specific capacitance (Fg^{-1})	Loading mass ($mgcm^{-2}$)	Ref
TiO_2 nanotube	Anodization	Galvanostatic Test	10 $uAcm^{-2}$	2.6	19.2	0.135	17
Hydrogenated TiO_2 nanotube	Anodization & annealing under H_2	Cyclic voltammetry	10 mVs^{-1}	14.95	8.5	0.01	18
H-doped TiO_2 nanotube	Anodization & electrochemical doping	Galvanostatic Test	50 $uAcm^{-2}$	5.42	-	-	19
Reduced TiO_2 nanotube	Anodization & electrochemical reduction	Galvanostatic Test	10 $uAcm^{-2}$	0.949	-	-	20
Nitridated Hollow TiO_2	Sol-gel method	Cyclic Voltammetry	10 mVs^{-1}	2.48	-	-	21
TiO_2 dendrite	Electrochemical deposition	Cyclic voltammetry	5 mVs^{-1} 10 mVs^{-1}	34.2 29.4	28.5 24.5	1.2	**This work**

a

This research was done at the KANEKA/SKKU Incubation Center and financially supported by Kaneka Corp. in Japan and by the Basic Science Research Program through the National Research Foundation of Korea Grant, funded by the Ministry of Science, ICT & Future Planning (2009-0083540).

Notes and references

School of chemical Engineering, Sungkyunkwan University, Suwon, Republic of Korea. Fax: +82 31 299 4711; Tel: +82 31 290 7326; E-mail: yklee@skku.edu

† Electronic Supplementary Information (ESI) available: Detailed experimental process and supplementary data. See DOI: 10.1039/b000000x/

1 S. H. Nam, H.-S. Shim, Y.-S. Kim, M. A. Dar, J. G. Kim, *ACS Appl. Mater. Interfaces*. 2010, **7**, 2046; M. Xia, Q. Zhang, H. Li, G. Dai, H. Yu, T. Wang, B. Zou, Y. Wang, *Nanotechnology*., 2009, **20**, 055605; A. Tanaka, Y. Nishino, S. Sakaguchi, T. Yoshikawa, K. Imamura, K. Hashimoto, H. Kominami, *Chem. Comm*., 2013, **49**, 2551

2 Z. Sun, T. Liao, Y. Dou, S. M. Hwang, M.-S. Park, L. Jiang, J. H. Kim, S. X. Dou, *Nature Commun*., 2014, **5**, 3813; Z. Sun, J. H. Kim, Y. Zhao, F. Bijarbooneh, V. Malgras, Y. Lee, Y.-M. Kang, S. X. Dou, *J. Am. Chem. Soc*., 2011, **133**, 19314; F. H. Bijarbooneh, Y. Zhao, Z. Sun, Y.-U. Heo, V. Malgras, J. H. Kim, S. X. Dou, *APL Mater*., 2013, **1**, 032106.

3 C.-T. Yip, M. Guo, H. Huang, L. Zhou, Y. Wang, C. Huang, *Nanoscale*, 2012, **4**, 448

4 V.-M . Guerin, T. Pauporte, Energy Environ. Sci., 2011, **4**, 2971

5 J. Duay, S. A. Sherrill, Z. Gui, E. Gillette, S. B. Lee, ACS Nano, 2013, **7**, 1200; C. Yilmaz, U. Unal, *Electrochim. Acta*, 2014, **123**, 405.

6 F. Zhuge, J. Qiu, X. Li, X. Gao, X. Gan, W. Yu, *Adv. Mater*., 2011, **23**, 1330; D. Wang, L. Zhang, W. Lee, M. Knez, L. Liu, *Small*, 2013, **9**, 1025; J. Lei, W. Li, X. Li, L. Zeng, *J. Power Sources*, 2013, **242**, 838; J.-Y. Liao, B.-X. Lei, H.-Y. Chen, D.-B. Kuang, C.-Y. Su, *Energy Environ. Sci*., 2012, **5**, 5750; Z.-Y. Yuan, T.-Z. Ren, B.-L. Su, *Adv. Mater*., 2003, **15**, 1462.

7 C.-C. Hu, H.-C. Hsu, K.-H. Chang, *J. Electrochem. Soc*., 2012, **159**, D418; C.-C. Huang, H.-C. Hsu, C.-C. Hu, K.-H. Chang, Y.-F. Lee, Electrochim. Acta, 2010, 55, 7026.

8 C. Natarajan, G. Nogami, *J. Electrochem. Soc*., 1996, **143**, 1547; M.-S. Wu, M.-J. Wang, J.-J. Jow, W.-D. Yang, C.-Y. Hsieh, H.-M. Tsai, *J. Power Sources*, 2008, **185**, 1420.

9 M. V. Mandke, S.-H. Han, H. M. Pathan, *Crystengcomm*, 2012, **14**, 86; Z. Jiang, Y. Lin, Z. Xie, *Mater. Chem. Phys*., 2012, **134**, 762; L. D. Rafailovic, D. M. Minic, H. P. Karnthaler, J. Wosik, T. Trisovic, G. E. Nauer, *J. Electrochem. Soc*., 2010, **157**, D295.

10 X. Zhang, B. Yao, L. Zhao, C. Liang, L. Zhang, Y. Mao, *J. Electrochem. Soc*., 2001, **148**, G398; R. Liu, F. Wong, W. Duan, A. Sen, *Adv. Mater*., 2013, **25**, 6997.

11 J. Dong, H. Zheng, X. Yan, Y. Sun, Z. Zhang, *Appl. Phys. Lett*., 2012, **100**, 051112.

12 P.-C. Hsu, S.-K. Seol, T.-N. Lo, C.-J. Liu, C.-Li. Wang, C.-S. Lin, Y. Hwu, C. H. Chen, L.-W. Chang, J. H. Je, G. Margaritondo, *J. Electrochem. Soc*., 2008, **155**, D400.

13 S. H. Lee, H. Lee, M. Cho, J.-D. Nam, Y. Lee, *J. Mater. Chem. A*, 2013, **1**, 14606.

14 D. Pan, H. Huang, X. Wang, L. Wang, H. Liao, Z. Li, M. Wu, *J. Mater. Chem. A*, 2014, **2**, 11454.

15 P. Zhang, C. Shao, Z. Zhang, M. Zhang, J. Mu, Z. Guo, Y. Sun, Y. Liu, *J. Mater. Chem.*, 2011, **21**, 17746.

16 J. Yan, Y. Xiao, G. Ning, T. Wei, Z. Fan, *RSC Adv*., 2013, **3**, 2566.

17 M. Salari, S. H. Aboutalcbi, A. T. Chidembo, I. P. Nevirkovets, K. Konstantinov, H. K. Liu, *Phys. Chem. Chem. Phys*., 2012, **14**, 4770.

18 X. Lu, G. Wang, T. Zhai, M. Yu, J. Gan, Y. Tong, Y. Li, *ACS Nano*, 2012, **12**, 1690.

19 H. Wu, D. Li, X. Zhu, C. Yang, D. Liu, X. Chen, Y. Song, L. Lu, *Electrochim. Acta*, 2014, **116**, 129.

20 H. Zhou, Y. Zhang, *J. Power Sources*, 2013, **219**, 128.

21 G. D. Moon, J. B. Joo, M. Dahl, H. Jung, Y. Yin, *Adv. Funct. Mater*., 2014, **24**, 848.